Journal Pre-proof

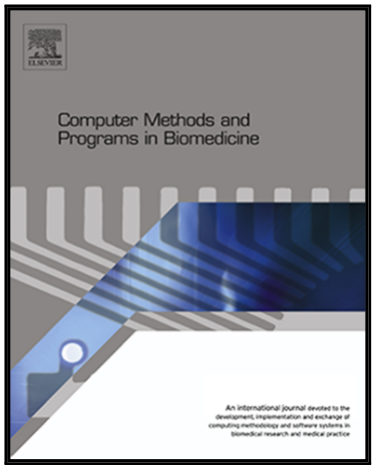

Correlation-based ECG Artifact Correction from Single Channel EEG using Modified Variational Mode Decomposition

Chinmayee Dora, Pradyut Kumar Biswal

PII: S0169-2607(19)30291-3
DOI: https://doi.org/10.1016/j.cmpb.2019.105092
Reference: COMM 105092

To appear in: *Computer Methods and Programs in Biomedicine*

Received date: 28 February 2019
Revised date: 11 September 2019
Accepted date: 23 September 2019

Please cite this article as: Chinmayee Dora, Pradyut Kumar Biswal, Correlation-based ECG Artifact Correction from Single Channel EEG using Modified Variational Mode Decomposition, *Computer Methods and Programs in Biomedicine* (2019), doi: https://doi.org/10.1016/j.cmpb.2019.105092

Highlights

- In the manuscript, modified VMD (mVMD) technique is used for ECG corrupted EEG signal decomposition. mVMD is useful for signal decomposition when signal contains correlation properties, which is the case for ECG related components.
- A simple correlation principle is able to identify the ECG related band limited mode functions (BLIMFs).
- From the identified ECG related BLIMFs ECG reference is estimated. The R-peaks could be identified and suppressed without any thresholding in the estimated reference ECG, as the epoch is very short.
- Rather discarding the identified ECG related BLIMFs, suppression of R-peaks helps to retain the low amplitude fluctuations, which may belong to source EEG signal.
- The proposed algorithm is able to correct the artifact with least distortion to the brain frequency bands.
- The correlation factor obtained by the proposed algorithm for actual EEG signal to estimated EEG signal is 97% without using a reference ECG channel.
- The proposed mVMD based algorithm is less computationally intensive than EEMD algorithm.

Correlation-based ECG Artifact Correction from Single Channel EEG using Modified Variational Mode Decomposition

Chinmayee Dora, Pradyut Kumar Biswal*

Dept. of Electronics & Telecommunication Engineering, International Institute of Information Technology, Bhubaneswar, India

Abstract

- *Background and objective:* Ambulatory based healthcare system use limited electrodes for electroencephalogram (EEG) acquisition at concerned electrode position, to minimize the instrumentation and computational complexity. But, again the possibility of contamination is inevitable depending on the electrode position on the scalp. This paper proposes an electrocardiogram (ECG) artifact correction algorithm in the absence of coherent ECG for automatic analysis/diagnosis of the acquired contaminated single channel EEG signal.

- *Methods:* The proposed algorithm uses an enhanced and modified version of signal decomposition i.e. modified variational mode decomposition (mVMD) to obtain band limited intrinsic mode functions (BLIMFs) from EEG epoch. The mVMD is found to be useful when the signal contains properties that are correlated. Further, exploiting the correlation among the obtained mode functions the ECG artifact components are identified. An ECG reference is estimated and QRS complexes are suppressed. The effective EEG reconstruction is performed by simply adding the remaining BLIMFs to QRS complex suppressed estimated reference. This is owing to the robust reconstruction feature provided by mVMD.

*Corresponding author

Email addresses: chinmayee.dora@gmail.com (Chinmayee Dora), pradyut@iiit-bh.ac.in (Pradyut Kumar Biswal)

Preprint submitted to Computer Methods & Programs in Biomedicine September 28, 2019

- *Results:* Upon the comparative evaluation for both real and semi-simulated dataset, the proposed algorithm is providing less distortion to the EEG brain activity frequency bands, and is also less computationally intensive than the existing Ensembled empirical mode decomposition (EEMD) based algorithm that requires ECG reference channel. Evaluation of semi-simulated dataset obtained an average correlation of 97% between EEG signals before contamination and after correction of ECG artifact.

- *Conclusion:* The proposed algorithm efficiently corrects the ECG artifact from EEG while overcoming the limitations such as, (1) requirement of a reference ECG channel, (2) requirement of R-R interval or amplitude thresholding for QRS complex identification.

Keywords:
EEG, ECG, artifact, modified VMD, EEMD, Correlation.

1. Introduction

Electroencephlalogram (EEG) is a low cost non-invasive technique for long term monitoring of brain activity with high temporal resolution. Hence, it is widely used for studying the brain function and pathology. However, during acquisition, recorded EEG often get contaminated by other non- cerebral biological signals from electrocardiogram (ECG), electrooculogram (EOG) and Electromyogram (EMG) signals. The sensitive EEG electrodes often pick up the ECG signals for its high amplitude and proximity to the heart [1], and contaminate the corresponding EEG recordings. The quasi-periodic high energy QRS complexes appears in the EEG recordings in various strengths depending on the electrode location on the scalp or physiology of subject itself.

Several approaches are proposed for ECG artifact removal, either using multi-channel EEG or single channel EEG. The multi-channel EEG approach uses blind source separation (BSS) techniques like independent component analysis (ICA) or principle component analysis (PCA) [2–4]. For recent advancement of health-care systems from hospital focused services to ambulatory focused services need minimization of instrumentation and computational complexity [5]. Also, single channel EEGs are used for brain function analysis [6]. This can be facilitated by EEG data acquisition using limited

electrodes at the concerned brain surface. In most of these cases, coherent ECG is absent. Hence, this paper focuses on ECG artifact removal from the EEG using single channel approaches. [7–11] are some of the single channel approaches proposed in the literature. Park et. al. [7] and Jiang et. al. [8] used the Teager-Kaiser energy operator and wavelet respectively to identify the ECG QRS complexes present in EEG, where the estimation of R- interval is essential for peak identification. The elimination of ECG artifact in above mentioned algorithms are achieved by modified ensembled average subtraction and weighted subtraction respectively. Waser et. al.[9] used a reference ECG for QRS peak identification, using several R-interval and amplitude thresholds to create an ideal regression reference for contaminated EEG signal. Source decomposition methods like empirical mode decomposition (EMD) and ensembled EMD (EEMD) are used by [10] and [11] respectively for ECG artifact removal from EEG. The significance of source decomposition over wavelets is that, it does not need any prior knowledge about the signal of interest. Navarro et. al. [10] decomposed the EEG signal using EMD and then adaptively filtered the EEG component using a reference ECG. Patel et. al. [11] used EEMD upon the reference ECG signal along with PCA to obtain a clean reference to regress with contaminated EEG signal. The major limitations of all above mentioned algorithms are:

1. Requirement of a reference ECG channel.
2. Estimation of R intervals for identifying QRS complexes present in EEG along with amplitude thresholds.

Hence, this paper focuses on the ECG artifact removal from EEG signal to overcome the limitations mentioned above. The authors also proposed another algorithm [12] to address these limitations. This proposed algorithm uses a modified version of advanced signal decomposition algorithm called variational mode decomposition (VMD) [13] on EEG. VMD decomposes a time series with better tone detection and separation along with noise robustness than EMD and EEMD [14]. VMD is used in the literature for different applications like fault detection [15, 16], signal analysis [17–20], classification and prediction [21–23] and bio-medical signal processing [24–27] etc. Using a predefined set of parameters, VMD provides an effective signal decomposition. Here, in this paper a modified VMD (mVMD) approach is used for signal decomposition. Exploiting the correlation among the decomposed mode functions, the ECG related mode functions are identified. From the identified mode functions the ECG artifact is estimated, in which R peaks

are detected and suppressed. Then, the EEG signal is reconstructed from the QRS complex suppressed component and other remaining components.

The paper proceeds as follows, Section 2 discuses the different signal decomposition algorithms and concept of the mVMD in brief. Section 3 describes the proposed technique and illustrates the proposed algorithm. The dataset and performance indexes used for evaluation are discussed in section 4. Section 5 presents the performance evaluation results followed by a discussion in section 6. Finally a conclusion is presented in the section 7.

2. Signal decomposition: A brief discussion

2.1. Empirical mode decomposition (EMD) and Ensemble empirical mode decomposition (EEMD)

The EMD algorithm [28] assumes, any non-stationary and non-linear time series consists of intrinsic modes of oscillation. EMD algorithm identify these intrinsic oscillatory modes empirically using the characteristic time scales in the data, and then decompose the data accordingly. Considering signal oscillations at a very local level, EMD algorithm separates the time series into non-overlapping time scale components locally i.e. Intrinsic mode functions (IMFs). For the signal X(t) decomposition into its IMFs, the algorithm obeys two properties:

- The number of extrema and the number of zero crossing must be equal or differ at most by one;
- The mean value of each IMF is zero.

The algorithm can be summarized in the following steps:

i. In the time series, identify the local maxima and minima
ii. Using cubic splines interpolation deduce an upper and a lower envelope.
    - Subtract the mean envelope from the time series
    - Iterate until #{extrema} = #{zeroes} $\pm$ 1
iii. Subtract obtained Intrinsic Mode Function (IMF) from the time series
iv. Iterate on the residual

The major disadvantage of EMD is the mode mixing effect. This usually occur when the oscillations with different time scales are retained in one

intrinsic mode function (IMF), or the same time scale oscillations are distributed over different IMFs. To overcome the mode mixing effect, Wu and Huang [29] proposed an enhanced EEMD algorithm by adding a white gussian noise to the input signal. It enabled a better scale separation aptitude than the standard EMD algorithm. The EEMD adds different series of white noise into the signal in the iteration. As the noise added are different in each iteration, the resulting IMFs are uncorrelated with the corresponding IMFs from one iteration to another. With adequate number of iteration, the added noise is eliminated by ensembled averaging the IMFs obtained for different iterations as illustrated in Fig. 1. The algorithm for EEMD can be summarized in the steps below:

i. Generate $x^i(n) = x(n) + r_t^i(n)$ where $r_t^i(n), i = 1, 2, ..., I$ are series of white Gaussian noise for I iterations.
ii. Each $x^i(n)$ is decomposed by EMD algorithm to obtain K number of $IMF_k^i(n), k = 1, 2, ..K$.
iii. The ensembled average $IMF_k^i(n)'$ is obtained by $IMF_k^i(n)' = \frac{1}{I}\sum_{i=1}^{I} IMF_k^i(n)$

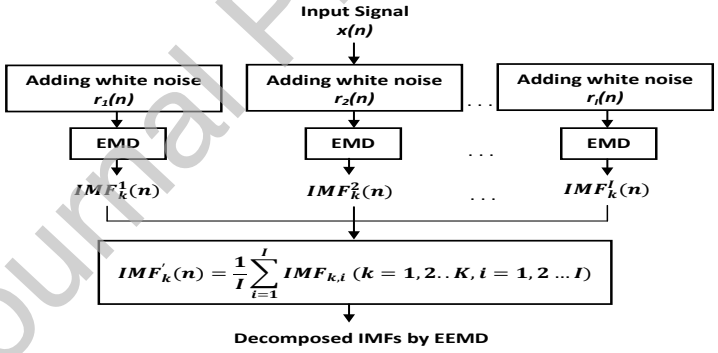

Figure 1: EEMD Algorithm flowchart

2.2. Variational mode decomposition

Unlike EMD and EEMD, VMD can decompose non-stationary multicomponent time series X into discrete number of quasi-orthogonal sub-signals x_k non-recursively. These sub-signals or IMFs are compact around a center frequency ω_k with limited bandwidth. The VMD algorithm to assess the bandwidth of time series is as follows:

i. for each mode x_k, using the Hilbert transform a unilateral frequency spectrum is obtained. The associated analytic signal is computed.
ii. The mode's frequency spectrum is shifted to the baseband by mixing with an exponential tuned to the respective estimated centre frequency, for each mode.
iii. The bandwidth is estimated through Gaussian smoothness of the demodulated signal.

The modes obtained by VMD shows less instantaneous frequency fluctuations in comparison to EMD and EEMD. VMD outperforms EMD and EEMD in terms of tone detection, tone separation and noise robustness along with signal reconstruction [13].

Stating a simple denoising problem, where X_0 is observed signal of the actual signal X affected by additive zero mean gaussian noise is given by,

$$X_0 = X + \eta \tag{1}$$

Recovering X is a typical ill-posed inverse problem. To recover the input signal X from the observed signal X_0, Tikhonov Regularization is used as a solution of the minimization problem [30, 31] , as follows:

$$X_{min} \left\{ \|X - X_0\|_2^2 + \alpha \|\partial_t X\| \right\} \tag{2}$$

from which Euler-Lagrange equations could be obtained and solved in Fourier domain:

$$\hat{X}(\omega) = \frac{\hat{X}_0}{1 + \alpha\omega^2} \tag{3}$$

where, $\hat{X}(\omega) \rightarrow F\{X(.)\}(\omega) \rightarrow 1/\sqrt{2\pi} \int_{\mathbb{R}} f(t) e^{j\omega t} dt$, with $j^2 = -1$, is the Fourier transform of the signal $X(t)$. The solution correspond to a convolution with Weiner filter, with α as the variance of the white noise and $1/\omega^2$ as lowpass power spectrum of signal.

VMD algorithm is the generalized form of Weiner filter with adaptive and multiple band method. It decomposes the real values signal X into a discrete number of components or modes, where each mode x_k is compact around a center frequency ω_k. These band limited IMFs (BLIMFs) are obtained by solving a constrained variational problem described mathematically :

$$\min_{x_k . \omega_k} \left\{ \sum_{k=1}^{K} \left\| \partial_t \left[\left(\delta_t + \frac{j}{\pi t} \right) * x_k(t) \right] e^{-j\omega_k t} \right\|_2^2 \right\} \tag{4}$$

subject to $\sum_{k=1}^{K} x_k = X$

where $x_k \; for \; k = 1, 2, ..K$ are the BLIMFs of center frequency ω_k obtained by decomposition, with K defined *a priori*.

The constrain of equation 4 is addressed by using a quadratic penalty term and Langrangian multiplier (λ). Hence, with δ_t as Dirac distribution and $*$ as convolution operator the augmented Langrangian equation is given by,

$$\begin{aligned} \mathfrak{L}\left(\{x_k\},\{\omega_k\},\lambda\right) &= \alpha \sum_{k=1}^{K} \left\| \partial_t \left[\left(\delta_t + \frac{j}{\pi t} \right) * x_k(t) \right] e^{-j\omega_k t} \right\|_2^2 \\ &\quad + \left\| X(t) - \sum_{k=1}^{K} x_k(t) \right\|_2^2 + \left\langle \lambda(t), X(t) - \sum_{k=1}^{K} x_k(t) \right\rangle \end{aligned} \quad (5)$$

Where α is the balancing parameter for the data fidelity constraint. Here the embedded Wiener filter in the VDM algorithm makes it insusceptible to sampling and noise. Alternate Direction Method of Multipliers (ADMM) [32] is used to estimate the saddle point of equation 5 corresponding to the solution of equation 4, with convergence tolerance of ε, where the convergence criterion is defined by,

$$\sum_{k} \left(\frac{\left\| \hat{x}_k^{n+1} - \hat{x}_k^{n} \right\|_2^2}{\left\| \hat{x}_k^{n} \right\|_2^2} \right) < \varepsilon \quad (6)$$

The k^{th} mode estimate is updated using equation 12 and equation 13 defined by

$$\hat{x}_k^{n+1}(\omega) = \frac{\hat{X}(\omega) - \sum_{i<k} \hat{x}_i^{n+1}(\omega) - \sum_{i>k} \hat{x}_i^{n}(\omega) + \frac{\hat{\lambda}^n(\omega)}{2}}{1 + 2\alpha(\omega - \omega_k^n)^2} \quad (7)$$

$$\omega_k^{n+1} = \frac{\int_0^\infty \omega \left| \hat{x}_k^{n+1}(\omega) \right|^2 d\omega}{\int_0^\infty \left| \hat{x}_k^{n+1}(\omega) \right|^2 d\omega} \quad (8)$$

2.3. Modified VMD (mVMD)

The original proposed VMD uses Tikhonov Regularization for reconstruction of input signal. While, the mVMD approach [20] uses Elasticnet Regression which is a convex combination of Ridge and Lasso, combining the

penalties of both regression methods linearly [33]. When signal contains properties that are correlated, this type of regression is useful. The ECG components present in EEG signal shows correlation among them than the EEG related components. To overcome the limitation of Lasso regression which has l_1 term, a quadratic penalty term is used. Hence, the minimization problem of equation 2 is rewritten as,

$$X_{min}\left\{\|X - X_0\|_2^2 + \alpha\|\partial_t X\|_2^2 + \beta\|\partial_t X\|_1\right\} \tag{9}$$

with solution of the minimization problem as,

$$\hat{X}(\omega) = \frac{\hat{X}_0}{1 + \alpha\omega^2 + \beta j\omega} \tag{10}$$

The quadratic penalty term present makes the cost function strictly convex, hence it provides a single, global minimum. The augmented Langrangian equation is given by,

$$\begin{aligned}\mathfrak{L}\left(\{x_k\},\{\omega_k\},\lambda\right) &= \alpha\sum_{k=1}^{K}\left\|\partial_t\left[\left(\delta_t + \frac{j}{\pi t}\right) * x_k(t)\right]e^{-j\omega_k t}\right\|_2^2 \\ &\quad + \beta\sum_{k=1}^{K}\left\|\partial_t\left[\left(\delta_t + \frac{j}{\pi t}\right) * x_k(t)\right]e^{-j\omega_k t}\right\|_1 \\ &\quad + \left\|X(t) - \sum_{k=1}^{K} x_k(t)\right\|_2^2 + \left\langle\lambda(t), X(t) - \sum_{k=1}^{K} x_k(t)\right\rangle\end{aligned} \tag{11}$$

The updated k^{th} mode estimate from equation 11 is defined by,

$$\hat{x}_k^{n+1}(\omega) = \left[\hat{X}(\omega) - \sum_{i<k}\hat{x}_i^{n+1}(\omega) - \sum_{i>k}\hat{x}_i^{n}(\omega) + 2\beta(\omega - \omega_k^n) + \frac{\hat{\lambda}^n(\omega)}{2}\right]\frac{1}{1 + 2\alpha(\omega - \omega_k^n)^2} \tag{12}$$

$$\omega_k^{n+1} = \frac{\int_0^\infty \omega\left|\hat{x}_k^{n+1}(\omega)\right|^2 d\omega}{\int_0^\infty \left|\hat{x}_k^{n+1}(\omega)\right|^2 d\omega} \tag{13}$$

The mVMD improves the IMF separation in components with correlation property while center frequency update remaining the same as VMD.

3. Proposed algorithm

The ECG artifacts dominantly contaminate the EEG recordings from temporal and auricular lobes. The ECG contamination in EEG occurs for superimposition of QRS complexes of ECG over EEG signal due to its high energy content. The other parts of the ECG signal get submerged in EEG for their low amplitude [34]. Hence the contaminated EEG appears with the characteristic ECG quasi-periodic spikes in bi-phasic or tri-phasic form changing the EEG morphologically which could mislead the diagnosis/analysis. To highlight the effect of QRS complex of ECG signal on EEG, an ECG signal at SNR 10 (i.e. approx. 10% of the true ECG) is added to an EEG segment. The Fig. 2 shows a segment of ECG superimposed EEG. It could be observed that when the ECG segment is superimposed on EEG, the QRS complex alters the EEG segment, while other parts of EEG retains its characteristics. The effect of ECG contamination on EEG is analyzed in detail using a case study in discussion section.

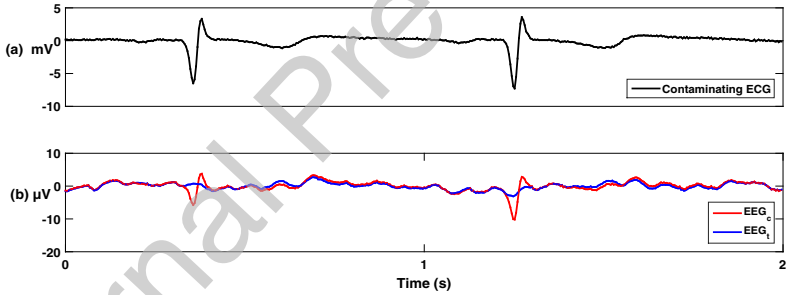

Figure 2: *(a)* Contaminating ECG, *(b)* True EEG and Contaminated EEG

The proposed algorithm is able to identify and eliminate ECG artifact from EEG using the quasi-periodic nature of QRS waves without estimating the R-R intervals. The ECG related components for the presence of QRS waves have a high correlation, where as the EEG signal components being non stationary in nature have a very low correlation with each other. The algorithm involves four stages: Application of mVMD on input EEG, identifying the ECG components from decomposed BLIMFs and estimating ECG reference, identification and correction of QRS complex in estimated ECG reference, and reconstruction of artifact free EEG from the QRS complex corrected ECG components and remaining BLIMFs. The four stages are detailed below.

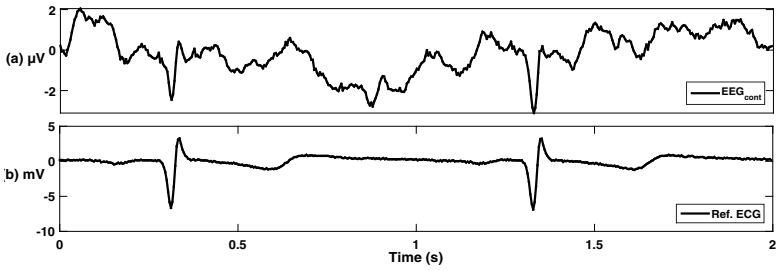

Figure 3: *(a)* Input ECG Contaminated EEG, *(b)* Reference ECG

(i) ***Application of mVMD on input EEG***: The features of VMD analyzed in [14] established that,

(a) VMD can retrieve non uniform samples perfectly over EMD/EEMD.

(b) Unlike EMD/EEMD, equivalent filter bank property of VMD do not change with increasing non-stationarity of the signal, i.e. the limited bandwidth of the BLIMFs remain same irrespective non-stationarity of EEG signal.

(c) The EEG signal is completely random in nature; hence the power distribution of the signal over the frequency band is assumed to be Gaussian. Whereas, ECG signal power range lies below 30 Hz, with maximum power concentrated around the QRS complex [35]. Hence the high energy QRS complexes in the contaminated EEG signal could be treated as impacts.

Hence, mVMD of EEG epoch by choosing suitable α and β, solves the purpose of separating EEG components from ECG components. mVMD is applied on an epoch of 2s of the contaminated EEG (EEG_c). An input epoch is shown in Fig.3 along with the reference contaminating ECG. The parameter α and the parameter β is set to 1000 and 0.01 respectively [33]. The initialization parameter is set to 1 for uniformly distributed center frequencies (ω_k). The number of decomposed BLIMFs 'K'is set to 12. The choice for number of modes (K) as 12 established heuristically permits the decomposition to an extent, where the artifact components and EEG components could be well separated. Hence, a correlation could be established to separate the ECG components with their quasi periodic waves. The analysis for the chosen K value is detailed in the section 6. The Fig. 4 shows the obtained BLIMFs.

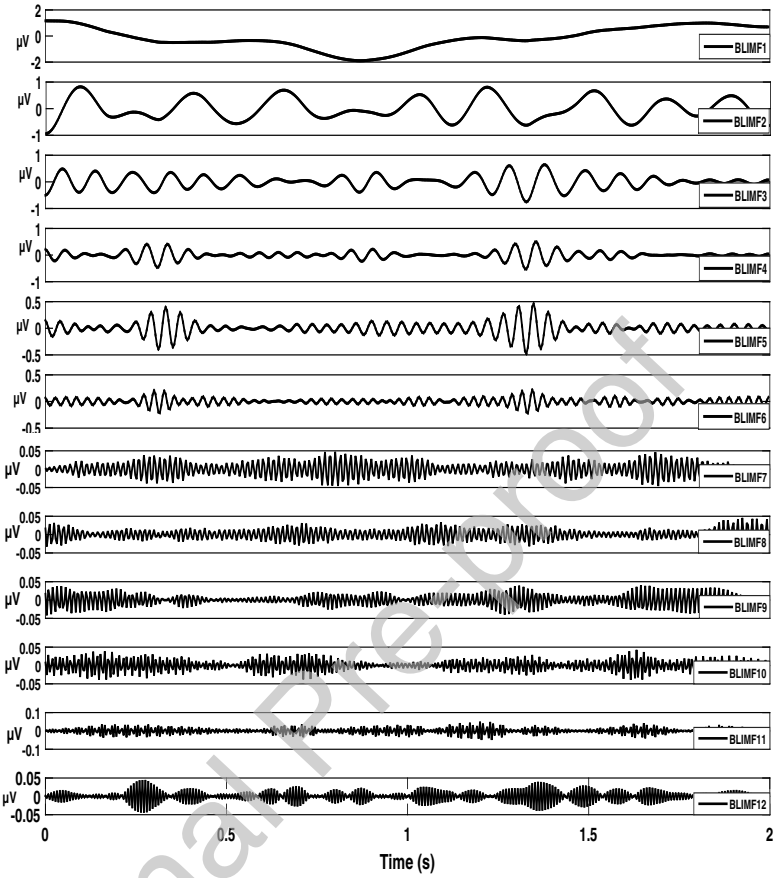

Figure 4: Variational mode decomposition of ECG contaminated EEG (BLIMF 1 to 12)

(ii) ***Identification of ECG related BLIMFs***: The BLIMFs which contains the ECG components exhibit a quasi- periodic pattern due to the QRS peaks. Hence to enhance the pattern, the obtained BLIMFs are squared and then convolved with a triangular membership function. The Fig. 5 shows the BLIMFs after squaring and convolution. For the automatic identification of quasi-periodic patterned BLIMFs, one to one correlation matrix is obtained, not taking the self correlation of BLIMFs into account. The BLIMFs containing ECG components are highly correlated, where as the EEG components are less correlated for their non-stationary nature. The Fig. 6 shows the correlation matrix plot. The BILMFs which are correlated by 85% of maximum correla-

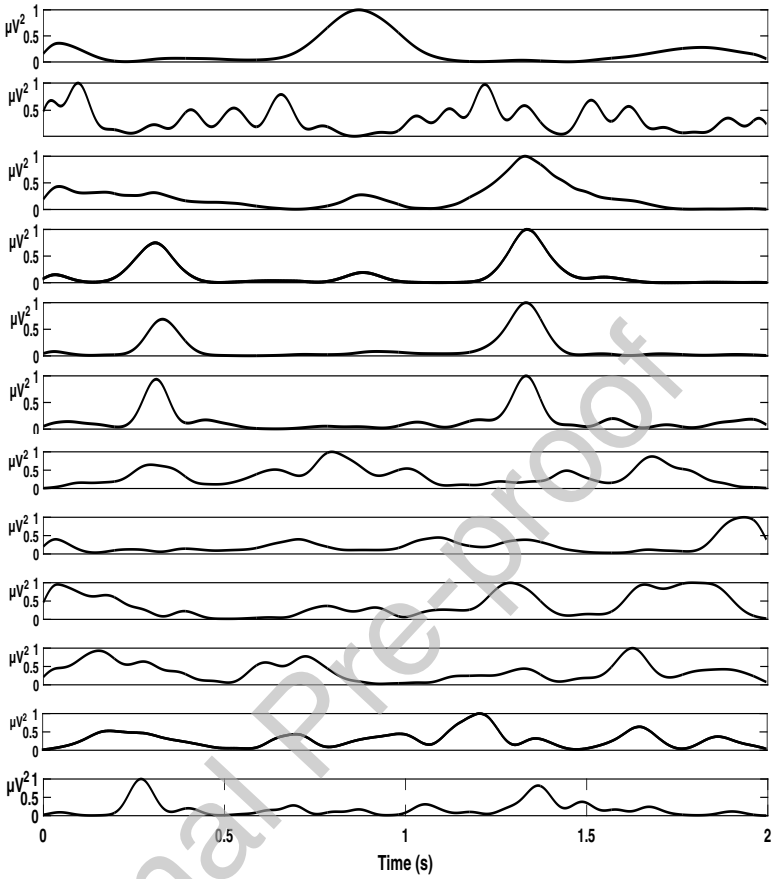

Figure 5: BLIMF 1 to 12 after squaring and convolution

tion in the neighborhood of maximum correlated BLIMFs are identified as ECG related components. The threshold is determined heuristically for close proximity of ECG components among them. The correlation among the BLIMFs are illustrated using Fig. 6. For the segment of contaminated EEG considered for graphical illustration, BLIMF4, BLIMF5 and BLIMF6 shows highest correlation among themselves. Hence, they are identified as the ECG artifact related components. From the identified artifact related BLIMFs, an ECG reference is estimated. The estimated ECG components are shown in the Fig. 7.

(iii) ***Identification and Suppression of QRS complexes in estimated ECG reference***: The EEG signals mostly corrupted by the

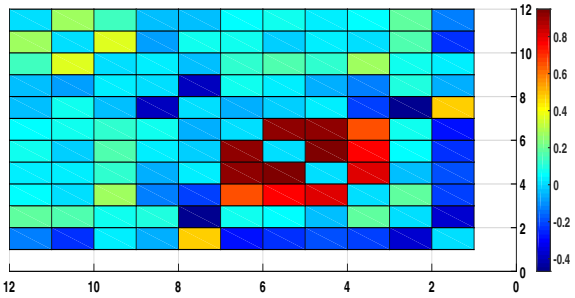

Figure 6: Correlation among BLIMFs: 2-D plot

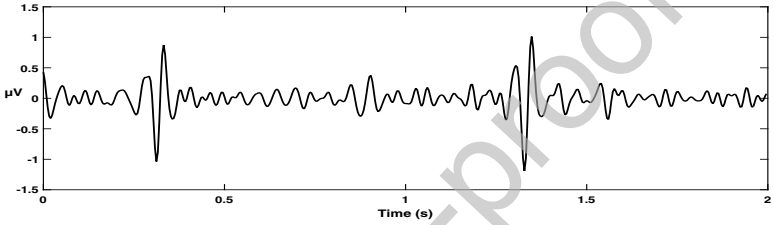

Figure 7: Estimated ECG reference from BLIMFs

high energy QRS spikes of ECG signal, which appears as quasi periodic spikes in EEG. Hence, by suppressing these QRS complexes in EEG, artifact correction could be achieved. To suppress the QRS complexes from the estimated ECG reference, it is squared first. Then the squared ECG reference get enhanced at peaks. Taking a shorter epoch like 2s, gives the advantage of locating the peaks without any thresholding in time or amplitude. Again, considering the case of Tachycardia (bpm near about 100) to Bradycardia (bpm<60) or Arrythmia [36], the 2s epoch will have minimum 1 QRS wave to maximum 2 to 3 QRS waves. Hence it could be assumed that no prior knowledge about the ECG type that is contaminating the EEG is required. As the epoch is short, Matlab 'findpeaks' command could identify the QRS complexes. The average QRS duration is about 100 ms to 120 ms. By suppressing 60 ms before and after the peak location, from the estimated ECG reference QRS complexes are eliminated. The Fig. 8 shows squared estimated ECG reference, QRS complex located ECG reference and QRS complex eliminated estimated ECG reference.

(iv) ***Reconstruction of EEG***: Identifying and suppressing the QRS complexes in the estimated reference ECG, the EEG signal components

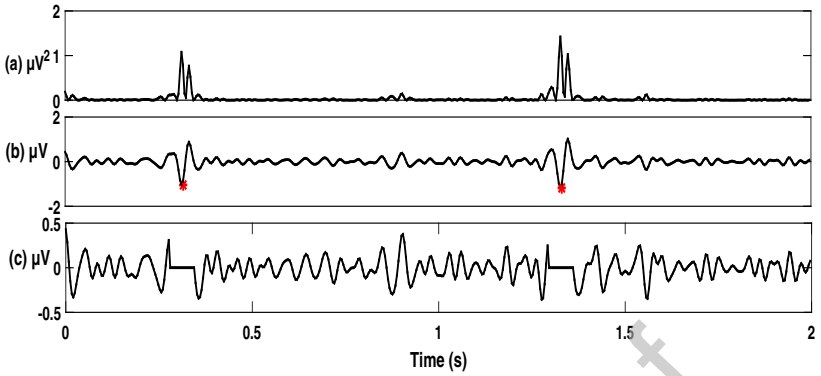

Figure 8: a) Squared estimated ECG reference,b) QRS complex located ECG reference, c) QRS complex eliminated estimated ECG reference.

that could be present in the estimated ECG are retained. Hence providing least distortion to the original EEG signal. The artifact free EEG (EEG_e) is reconstructed from the remaining BLIMFs and the QRS complex suppressed estimated ECG. The Fig. 9 shows the artifact corrected EEG corresponding to the contaminated one. Results for another 2s excerpt of 'slp01am' record from the MIT/BIH dataset is shown in Fig. 10.

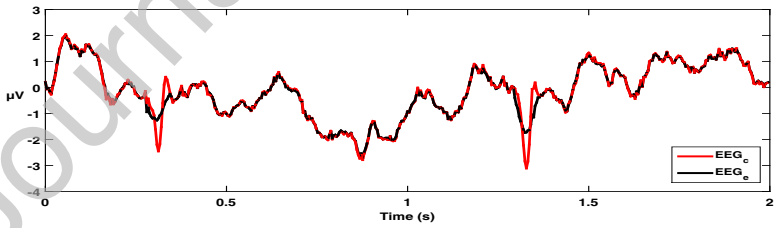

Figure 9: ECG artifact corrected EEG, excerpt from 'sub1' of Semi-simulated data

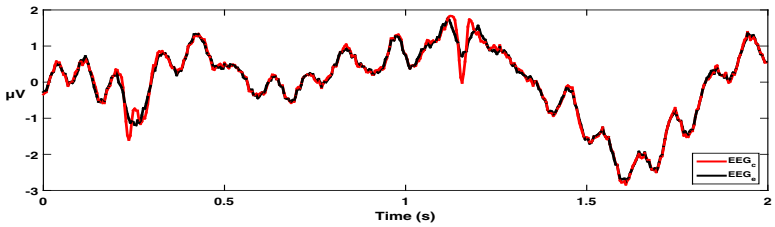

Figure 10: ECG artifact corrected EEG, excerpt from 'slp01am' of MIT/BIH Polysomnography data

4. Evaluation dataset and performance indexes

4.1. Evaluation dataset

In this study, two sets of EEG recordings i.e. experimental dataset and semi-simulated dataset are used as described below:

- *Experimental dataset:* Expermental dataset is taken from polysomnography database, availed by Massachusetts Institute of Technology recorded at Beth Israel Hospital (MIT/BIH). Randomly chosen 100s of each ECG contaminated EEG recordings from 'slp01am', 'slp01bm' and 'slp67xm' (i.e. a total of 300s) are used for algorithm evaluation [37, 38].

- *Semi-simulated dataset:* Ten random non-contaminated EEG (EEG_t) recordings of 100s each i.e. a total of 1000s EEG recording of normal subjects are obtained. These EEG recordings of C3-O1 electrode are from 'Challenge 2014 Training Set' of Physionet [38]. The obtained clean EEG data are contaminated by additive ECG noise with a fraction of λ as given in equation 14. Hence, to generate a semi-simulated EEG i.e. EEG_c, fraction λ is so adjusted that, the obtained SNR is 10 as per the equation 15 [39].

$$EEG_c = EEG_t + \lambda.ECG \tag{14}$$

$$SNR = \frac{RMS(EEG_t)}{RMS(\lambda.ECG)} \tag{15}$$

Where, RMS is defined as the root mean square energy of the signal. A segment of semi-simulated EEG (EEG_c) used for the algorithm evaluation is shown in the Fig.11.

Also, to validate the case study described in section 6, REM sleep segments of 10s each from 5 insomnia subjects and 5 normal subjects of cyclic alternating pattern (CAP) sleep data ('capslpdb') [38, 40] are used for evaluation of effect of ECG contamination on EEG. The EEG recordings of normal subjects are then contaminated by simulation and evaluated for artifact correction using the proposed algorithm.

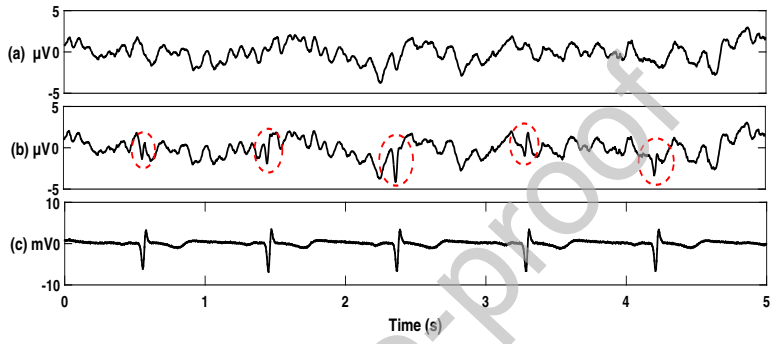

Figure 11: *Simulated EEG Data:(a)* Uncontaminated EEG, *(b)* Contaminated EEG, *(c)* Contaminating ECG

4.2. Performance indexes

Along with the graphical illustration, the performance parameters used to evaluate the proposed algorithm are:

- ΔPSD: The change in EEG signal power (ΔPSD)in the different frequency bands of brain activity i.e. Delta (0.5Hz- 4Hz), Theta (4Hz- 8Hz), Alpha (8Hz- 12Hz) and Beta (12Hz- 30Hz) before and after the ECG artifact removal. The ΔPSD is calculated using Welch's method and lower value of it suggest lower distortion introduced to the EEG_e after ECG artifact correction [41].

- Signal to artifact ratio (SAR) is to measure the extent of artifact removal by the algorithms [42]. SAR is calculated for both set of data as defined in the equation 16, where *std* is the standard deviation.

$$SAR = 10\ log\ \left(\frac{std(EEG_c)}{std(EEG_c - EEG_e)}\right) \tag{16}$$

- Correlation factor (C_f): A correlation factor measures the strength and direction of linearity between two signals. It is used to validate the correlation between the EEG_t and EEG_e for simulated EEG dataset. The correlation factor for variables p with mean $\bar{p}$ and q with mean $\bar{q}$ for a sample length of N is calculated as below:

$$C_f(p,q) = \frac{\sum_{i=1}^{N}(p_i - \bar{p})(q_i - \bar{q})}{\sqrt{\left(\sum_{i=1}^{N}(p_i - \bar{p})^2 \sum_{1}^{N}(q_i - \bar{q})^2\right)}} \tag{17}$$

5. Results

The results of the proposed algorithm are compared against EEMD based algorithm proposed by R. Patel et. al. [11]. Both the algorithms are implemented on MIT/BIH Polysomnography data. The change in power spectral density (ΔPSD) by Welch's method is estimated for a comparative performance evaluation. The ΔPSD for contaminated EEG and estimated EEG is calculated in different frequency bands of brain activity i.e. Delta (0.5Hz-4Hz), Theta (4Hz- 8Hz), Alpha (8Hz- 12Hz) and Beta (12Hz- 30Hz). The results obtained for ΔPSD shown in Table 1 is for MIT/BIH Polysomnography data.

Table 1: Comparative ECG removal performance using ΔPSD and SAR for MIT/BIH dataset

ΔPSD **for MIT/BIH Polysomnography Data**	**EEMD based Algorithm [11]**	**mVMD based Algorithm**
PSD_δ	0.396±0.51	0.378±0.53
PSD_θ	0.146±0.17	0.127±0.16
PSD_α	0.118±0.18	0.098±0.13
PSD_β	0.303±0.21	0.231±0.23
SAR	13.49±0.12	18.72±0.09

The Table 2 shows the comparative ΔPSD among the proposed method with EEMD based algorithm [11] and modified S-transform based algorithm [12] for semi-simulated EEG dataset with SNR 10. The proposed mVMD based technique is showing less change in ΔPSD than the other two algorithms. Hence, the proposed technique is optimally removing of the ECG

artifact with least distortion to the frequency bands of brain activity. For the statistical validation of the proposed algorithm, two sample t-test is performed on the results obtained by both the method. The proposed method found to be significant by p-value < 0.05 for the ΔPSD results obtained from both the method.

Table 2: Comparative ECG removal performance using ΔPSD for semi-simulated dataset at SNR 10

EEG Record	**Sub1**	**Sub 2**	**Sub 3**	**Sub 4**	**Sub 5**	**Sub 6**	**Sub 7**	**Sub 8**	**Sub 9**	**Sub 10**	**Mean ±std**
EEMD based Algorithm [11]											
PSD_δ	0.160	0.624	1.099	0.751	0.133	0.330	0.039	0.493	0.226	0.479	0.433±0.33
PSD_θ	0.108	0.255	0.200	0.212	0.180	0.417	0.143	0.251	0.188	0.523	0.248±0.13
PSD_α	0.031	0.178	0.250	0.157	0.247	0.028	0.213	0.257	0.325	0.523	0.220±0.14
PSD_β	0.485	0.274	0.256	0.423	0.355	0.238	0.811	0.381	0.618	0.686	0.453±0.2
Modified S-Transform based Algorithm [12]											
PSD_δ	0.441	0.262	0.113	0.482	0.498	0.384	0.050	0.159	0.392	0.323	0.311±0.16
PSD_θ	0.297	0.151	0.040	0.238	0.159	0.123	0.045	0.083	0.146	0.148	0.143±0.08
PSD_α	0.099	0.237	0.023	0.203	0.294	0.065	0.036	0.120	0.184	0.170	0.143±0.09
PSD_β	0.372	0.352	0.031	0.424	0.205	0.179	0.036	0.548	0.440	0.439	0.303±0.18
Proposed mVMD based Algorithm											
PSD_δ	0.340	0.137	0.061	0.057	0.371	0.110	0.072	0.623	0.118	0.040	**0.193±0.19**
PSD_θ	0.179	0.058	0.038	0.062	0.125	0.078	0.041	0.302	0.139	0.067	**0.109±0.08**
PSD_α	0.221	0.029	0.037	0.018	0.157	0.046	0.074	0.155	0.128	0.059	**0.092±0.07**
PSD_β	0.435	0.235	0.115	0.268	0.338	0.198	0.284	0.315	0.365	0.298	**0.285±0.09**

The SAR is calculated for results obtained with each record of semi-simulated data and compared against the EEMD based algorithm and modified S-transform based algorithm. The obtained improved SAR for the proposed algorithm also corroborating the fact of better performance, shown in the Table 3. Again, the EEMD based algorithm achieves a correlation factor of 99% using a reference ECG channel, while the proposed method achieves a correlation factor of 97% without using reference ECG channel.

Further the computational complexity is evaluated in terms of execution time. The execution time to decompose 10s EEG data length using mVMD and EEMD routine, and execution time for artifact correction using EEMD based algorithm, modified S transform based algorithm, and proposed algorithm is compared. The execution time is estimated using MATLAB environment, with 4GB RAM, Core 2Duo Processor with 2GHz clock frequency. As per the values in the Table 4, The proposed algorithm is found to be computationally less intensive over the EEMD based algorithm.

Table 3: Comparative ECG removal performance using SAR and C_f for semi-simulated dataset

EEG Records	EEMD based Algorithm [11]		Modified S-Transform [12] based Method		Proposed mVMD based Method	
	SAR	C_f	SAR	C_f	SAR	C_f
Sub 1	12.93	1.00	13.11	0.96	16.31	0.97
Sub2	15.92	0.99	13.32	0.96	17.86	0.97
Sub 3	7.25	0.99	16.68	0.98	19.44	0.98
Sub 4	8.98	0.99	11.79	0.95	15.66	0.98
Sub 5	12.10	1.00	12.39	0.95	14.72	0.97
Sub 6	13.81	1.00	14.70	0.96	19.76	0.95
Sub 7	16.51	0.99	16.99	0.99	20.74	0.96
Sub 8	11.78	0.99	15.27	0.98	17.28	0.95
Sub 9	10.60	1.00	11.56	0.94	16.22	0.97
Sub 10	10.18	0.99	17.70	0.97	19.98	0.97
Mean	**12.01**	**0.99**	**14.35**	**0.96**	**17.80**	**0.97**

Table 4: Comparative computational complexity in terms of execution time (in s) for 10s EEG data

Algorithm	Execution time (in s)
data decomposition using EEMD	146.41
data decomposition using mVMD	27.89
EEMD based Algorithm [11]	153.57
Modified S-transform based Algorithm [12]	0.442
mVMD based Algorithm	38.35

6. Discussion

6.1. Effect of ECG artifact on EEG: A case study

The pre-processing of EEG records with least distortion is essential for analysis purpose. Authors of [43] studied the effect of ECG artifact on EEG and deduced that ECG artifact affects the results of sleep stage classification. To further validate the same, a small case study is done. As per the study, subjects with chronic insomnia [44] have an enhanced mean PSD in Alpha (α)

(6.75-12.5Hz), Sigma (σ) (12.5-14.75Hz), and Beta (β) (14.75-30Hz) brain activity level, where as Theta (θ) (3.75-6.75Hz) activity level is lowered and Delta (δ) activity level is not affected in random eye movement (REM) sleep episode. The Table 5 shows the comparative mean PSDs of EEG in different frequency bands of 5 normal subjects to 5 subjects suffering from insomnia for REM sleep episodes.

Table 5: Mean PSDs in different brain frequencies for REM sleep of normal subjects and insomnia patients

Brain Activity Frequency bands	**PSD (Mean ± SD) of Normal Subjects**	**PSD (Mean ± SD) of Insomniac Subjects**
PSD_δ	0.1381±0.04	0.1232±0.02
PSD_θ	0.0500±0.02	0.0342±0.02
PSD_α	0.0489±0.01	0.0562±0.01
PSD_σ	0.0126±0.01	0.0175±0.01
PSD_β	0.0316±0.02	0.0474±0.01

To observe the ECG contamination effect on REM EEG signal, the normal EEG records are contaminated with ECG artifact and mean PSDs of different frequency bands are evaluated. Table 6 shows effect of ECG contamination to EEG, which enhance the brain activity level of α, σ and β frequency. These three frequency bands are spectrally similar with the QRS complex of ECG. This may misclassify the normal EEG as an insomnia patient when subjected to automatic classification. Further the EEGs are evaluated after ECG artifact removal using proposed mVMD based algorithm. The proposed algorithm shows the results close to the uncontaminated EEG, and could prevent it from misclassification.

6.2. Analysis

In this study, an effective approach for ECG artifact removal from single channel EEG is proposed. Short epochs of the non-stationary EEG can be decomposed to BLIMFs efficiently with application of mVMD. Adequate number of BLIMFs generation is possible as the decomposition level 'K' can be decided *a priori*, enabling full extraction of ECG artifact. To arrive at the number of decomosition modes, an analysis is performed using semi-simulated EEG signal with varying SNR ratio (i.e. SNR 8, 10, 12 and 15). The algorithm is implemented using different decomposition levels K (such as

Table 6: Mean PSDs for a set of normal EEG signals, after contamination and after artifact removal by proposed method

Mean ΔPSD	**Normal**	**Contaminated**	**After artifact removal**
PSD_δ	0.1381	0.1399	0.1390
PSD_θ	0.0500	0.0500	0.0480
PSD_α	0.0489	0.0571	0.0488
PSD_σ	0.0126	0.0160	0.0122
PSD_β	0.0316	0.0472	0.0321

8, 10, 12, 16, and 18). The cleaned EEG signal is analyzed using estimating normalized mean square error ($nmse$) between EEG before contamination and estimated EEG. $nmse$ is calculated as defined in the equation 18 [45].

$$nmse = \frac{\|(EEG_t - EEG_e)\|_2^2}{\|(EEG_t)\|_2^2} \tag{18}$$

The graph in Fig. 12 shows that for changing SNR level, the $nmse$ is higher when K is 8 or 10. For K value 12 onward the $nmse$ is almost unchanged. Hence, by increasing the number of modes more than 12, the results will not be affected but computation cost will increase.

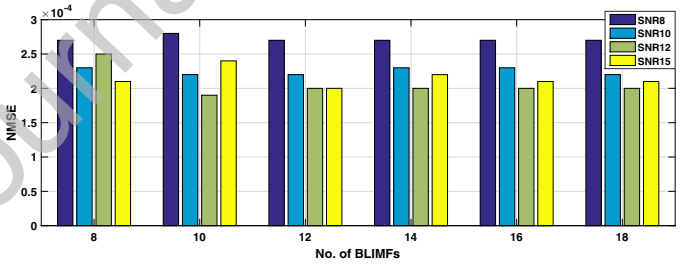

Figure 12: Comparative $nmse$ for varying SNR EEG signal with increasing K

The effective identification of ECG artifact is owing to the strong correlation among the ECG related BLIMFs. The mVMD algorithm updates the components combining the Lasso and Ridge regression parameter, where the center frequency update is same as VMD algorithm. Hence, in comparison to EMD and EEMD algorithm, mVMD algorithm can capture the relevant

center frequencies and separate the correlated BLIMFs more precisely. The EEG signals are usually corrupted by the high energy QRS complexes only. So, by generating adequate number of mode functions and identifying and suppressing the noisy QRS complexes, the reconstructed EEG signal approximate the artifact free EEG. Only suppressing the QRS complexes ensure no other low amplitude components which may belong to the EEG signal are compromised. The estimated EEG reconstruction is done from the remaining BLIMFs and QRS complex suppressed components. The quadratic penalty term in mVMD algorithm improves the convergence, where as the exact reconstruction is possible for the Langrangian multiplier which is enforcing the constraint on the mVMD. Hence, the reconstructed EEG approaches closely to the EEG before contamination.

7. Conclusion

A novel approach for single channel ECG artifact correction from EEG recordings is introduced in this paper. The major advantage of the proposed approach is ECG artifact identification from the decomposed BLIMFs requires neither reference ECG channel nor any R-interval and amplitude threshold estimation. mVMD works better when the signal contains property that are correlated. Hence, it provides better extraction of the ECG related components from contaminated EEG. Resembling ECG artifact BLIMFs due to the quasi-periodic pattern of QRS waves and uncorrelated EEG BLIMFs are aiding to the identification. The ECG identified BLIMFs are used to estimate the reference ECG, from where the QRS complexes are identified and suppressed. The reconstructed EEG from the remaining BLIMFs and QRS complex suppressed components, approaches the true EEG with least distortion. The influence of ECG artifact on EEG records for insomnia classification is discussed using a case study. The proposed algorithm is found to be less computationally intensive than EEMD based algorithm which also requires a reference channel. The proposed algorithm also found to be performing better in terms of ΔPSD while artifact correction along with improved SAR. Correlation based algorithm could work excellently for post signal processing of EEG recordings where the probability of ECG contamination is high. This may serve as an aid for pre-processing of EEG signals before subjected to any automatic analysis/diagnosis. The scope of this paper could be extended to investigate and eliminate the other physiological artifacts present in EEG.

References

[1] G. Dirlich, L. Vogl, M. Plaschke, F. Strian, Cardiac field effects on the EEG, Electroencephalography and Clinical Neurophysiology 102 (1997) 307–315.

[2] W. Zhou, Removal of ecg artifacts from eeg using ica, in: Proceedings of the Second Joint 24th Annual Conference and the Annual Fall Meeting of the Biomedical Engineering Society][Engineering in Medicine and Biology, volume 1, IEEE, pp. 206–207.

[3] S. Devuyst, T. Dutoit, P. Stenuit, M. Kerkhofs, E. Stanus, Cancelling ECG artifacts in EEG using a modified independent component analysis approach, EURASIP Journal on Advances in Signal Processing (2008) 1–14.

[4] M. B. Hamaneh, N. Chitravas, K. Kaiboriboon, S. D. Lhatoo, K. A. Loparo, Automated removal of EKG artifact from EEG data using independent component analysis and continuous wavelet transformation, IEEE Transactions on Biomedical Engineering 61 (2014) 1634–1641.

[5] X. Chen, A. Liu, J. Chiang, Z. J. Wang, M. J. McKeown, R. K. Ward, Removing muscle artifacts from EEG data: Multichannel or single-channel techniques?, IEEE Sensors Journal 16 (2016) 1986–1997.

[6] J. Camacho, V. Manian, Real-time single channel EEG motor imagery based brain computer interface, in: 2016 World Automation Congress (WAC), IEEE, pp. 1–6.

[7] H. J. Park, D. U. Jeong, K. S. Park, Automated detection and elimination of periodic ECG artifacts in EEG using the energy interval histogram method, IEEE Trans. Biomed. Eng. 49 (2002) 1526–1533.

[8] J. A. Jiang, M. J. C. C. F. Chao, R. G. Lee, R. L. C. G. Tseng, An automatic analysis method for detecting and eliminating ECG artifacts in EEG, Comput. Biol. Med. 37 (2007) 1660–1671.

[9] M. Waser, H. Garn, Removing cardiac interference from the Electroencephalogram using a modified Pan-Tompkins algorithm and linear regression, in: 35th Annual International Conference of IEEE EMBS,2013, pp. 2028–2031.

[10] X. Navarro, F. Poree, G. Carrault, ECG removal in preterm ECG combining empirical mode decomposition and adaptive filtering, in: Int. Conf. on Acoustics, Speech, and Signal Processing, IEEE, pp. 661–664.

[11] R. Patel, K. Gireesan, S. Sengottuvel, M. Janawadkar, T. Radhakrishnan, Common methodology for Cardiac and Ocular artifact suppression from EEG recordings by combining ensemble empirical mode decomposition with regression approach, Journal of Medical and Biological Engineering 37 (2017) 201–208.

[12] C. Dora, P. K. Biswal, Efficient detection and correction of variable strength ECG artifact from single channel EEG, Biomedical Signal Processing and Control 50 (2019) 168–177.

[13] K. Dragomiretskiy, D. Zosso, Variational mode decomposition, IEEE transactions on signal processing 62 (2014) 531–544.

[14] Y. Wang, R. Markert, Filter bank property of variational mode decomposition and its applications, Signal Processing 120 (2016) 509–521.

[15] Y. Wang, R. Markert, J. Xiang, W. Zheng, Research on variational mode decomposition and its application in detecting rub-impact fault of the rotor system, Mechanical Systems and Signal Processing 60 (2015) 243–251.

[16] P. D. Achlerkar, S. Samantaray, M. S. Manikandan, Variational mode decomposition and decision tree based detection and classification of power quality disturbances in grid-connected distributed generation system, IEEE Transactions on Smart Grid 9 (2018) 3122–3132.

[17] W. Liu, S. Cao, Y. Chen, Applications of variational mode decomposition in seismic time-frequency analysis, Geophysics 81 (2016) V365–V378.

[18] Y. Liu, G. Yang, M. Li, H. Yin, Variational mode decomposition denoising combined the detrended fluctuation analysis, Signal Processing 125 (2016) 349–364.

[19] R. Ram, M. N. Mohanty, Performance analysis of adaptive variational mode decomposition approach for speech enhancement, International Journal of Speech Technology 21 (2018) 369–381.

[20] B. O. Simsek, A. Akan, Frequency estimation for monophonical music by using a modified VMD method, in: 2017 25th European Signal Processing Conference (EUSIPCO), IEEE, pp. 1873–1876.

[21] Y. Zhang, K. Liu, L. Qin, X. An, Deterministic and probabilistic interval prediction for short-term wind power generation based on variational mode decomposition and machine learning methods, Energy Conversion and Management 112 (2016) 208–219.

[22] C. Yücelbaş, Ş. Yücelbaş, S. Özşen, G. Tezel, S. Küççüktürk, Ş. Yosunkaya, A novel system for automatic detection of K-complexes in sleep EEG, Neural Computing and Applications 29 (2018) 137–157.

[23] Ş. Yücelbaş, C. Yücelbaş, G. Tezel, S. Özşen, Ş. Yosunkaya, Automatic sleep staging based on SVD, VMD, HHT and morphological features of single-lead ECG signal, Expert Systems with Applications 102 (2018) 193–206.

[24] R. Tripathy, L. Sharma, S. Dandapat, Detection of shockable ventricular arrhythmia using variational mode decomposition, Journal of medical systems 40 (2016) 79.

[25] S. Pratiher, S. Mukhopadhyay, S. Hazra, R. Barman, G. Pasupuleti, N. Ghosh, P. K. Panigrahi, Early stage detection of precancer using variational mode decomposition and artificial neural network, in: Biophotonics: Photonic Solutions for Better Health Care VI, volume 10685, International Society for Optics and Photonics, p. 1068523.

[26] S. Nagineni, S. Taran, V. Bajaj, Features based on variational mode decomposition for identification of neuromuscular disorder using EMG signals, Health information science and systems 6 (2018) 13.

[27] M. T. Nguyen, B. Van Nguyen, K. Kim, Deep feature learning for sudden cardiac arrest detection in automated external defibrillators, Scientific reports 8 (2018) 17196.

[28] N. E. Huang, Z. Shen, S. R. Long, M. C. Wu, H. H. Shih, Q. Zheng, N.-C. Yen, C. C. Tung, H. H. Liu, The empirical mode decomposition and the hilbert spectrum for nonlinear and non-stationary time series

analysis, in: Proceedings of the Royal Society of London A: mathematical, physical and engineering sciences, volume 454, The Royal Society, pp. 903–995.

[29] Z. Wu, N. E. Huang, Ensemble empirical mode decomposition: a noise-assisted data analysis method, Advances in adaptive data analysis 1 (2009) 1–41.

[30] A. N. Tihonov, Solution of incorrectly formulated problems and the regularization method, Soviet Math. 4 (1963) 1035–1038.

[31] G. H. Golub, P. C. Hansen, D. P. O'Leary, Tikhonov regularization and total least squares, SIAM Journal on Matrix Analysis and Applications 21 (1999) 185–194.

[32] M. R. Hestenes, Multiplier and gradient methods, Journal of optimization theory and applications 4 (1969) 303–320.

[33] H. Zou, T. Hastie, Regularization and variable selection via the elastic net, Journal of the royal statistical society: series B (statistical methodology) 67 (2005) 301–320.

[34] J. M. Stern, Atlas of EEG patterns, Lippincott Williams & Wilkins, 2005.

[35] D. Chakrabarti, S. Bansal, ECG contamination of EEG signals: effect on entropy, Journal of clinical monitoring and computing 30 (2016) 119–122.

[36] D. H. Spodick, Normal sinus heart rate: Sinus tachycardia and sinus bradycardia redefined, American heart journal 124 (1992) 1119–1121.

[37] M. G. Ichimaru Y, Development of the polysomnographic database on cd-rom, Psychiatry and Clinical Neurosciences 53 (1999) 175–177.

[38] A. L. Goldberger, L. A. N. Amaral, L. Glass, J. M. Hausdorff, P. C. Ivanov, R. G. Mark, J. E. Mietus, G. B. Moody, C.-K. Peng, H. E. Stanley, PhysioBank, PhysioToolkit, and PhysioNet: Components of a new research resource for complex physiologic signals, Circulation 101 (2000 (June 13)) e215–e220. Circulation Electronic Pages: http://circ.ahajournals.org/content/101/23/e215.full PMID:1085218; doi: 10.1161/01.CIR.101.23.e215.

[39] X. Chen, A. Liu, H. Peng, R. Ward, A preliminary study of muscular artifact cancellation in single-channel EEG, Sensors 14 (2014) 18370–18389.

[40] M. G. Terzano, L. Parrino, A. Sherieri, R. Chervin, S. Chokroverty, C. Guilleminault, M. Hirshkowitz, M. Mahowald, H. Moldofsky, A. Rosa, R. Thomas, A. Walters, Atlas, rules, and recording techniques for the scoring of cyclic alternating pattern (cap) in human sleep, Sleep Medicine 2 (2001) 537 – 553.

[41] M. A. Klados, C. Papadelis, C. Braun, P. D. Bamidis, REG-ICA: A hybrid methodology combining blind source separation and regression techniques for the rejection of ocular artifacts, Biomedical Signal Processing and Control 6 (2011) 291 – 300. ITAB 2009.

[42] S. Khatun, R. Mahajan, B. I. Morshed, Comparative study of wavelet-based unsupervised ocular artifact removal techniques for single-channel EEG data, IEEE journal of translational engineering in health and medicine 4 (2016) 1–8.

[43] S. Yucelbas, C. Yucelbas, S. Ozsen, G. Tezel, M. Dursun, S. Kuccukturk, S. Yosunkaya, Effect on the classification results of ECG artifacts in full night sleep EEG.

[44] H. Merica, R. Blois, J.-M. Gaillard, Spectral characteristics of sleep EEG in chronic insomnia, European Journal of Neuroscience 10 (1998) 1826–1834.

[45] A. A. Poli, M. C. Cirillo, On the use of the normalized mean square error in evaluating dispersion model performance, Atmospheric Environment. Part A. General Topics 27 (1993) 2427–2434.

Appendix A. Algorithm

Algorithm 1: Algorithm for Proposed mVMD based ECG artifact removal

input : EEG_c : 2s epoch of Contaminated EEG ; f_s : Sampling frequency;

output : EEG_e : Artifact removed EEG ;

// Function $mVMD()$ performs modified Variational Mode Decomposition input data;
// Function $Square()$ squares the input;
// Function $Conv_{tri}()$ convolves the input with a Triangular membership function;

Initialization: $\alpha = 1000, \beta = 0.01, K = 12, indx = [\ ]; EEG_{est} = zeros(1, 2 * f_s)$;
$EEG_{cont} \leftarrow mVMD(EEG_{cont}, \alpha, \beta, K)$;
for $j \leftarrow 1$ **to** K **do**
    $BLIMF(j) \leftarrow Conv_{tri}(Square(BLIMF(j)))$
for $j \leftarrow 1$ **to** K **do**
    for $k \leftarrow 1$ **to** K **do**
        if $j \neq k$ **then**
            Calculate Correlation coefficient matrix C_{coff} of BLIMF(j) and BLIMF(k)
Calculate $max(C_{coff}) = C$ and find the corresponding j^{th} row and k^{th} column;
$indx \leftarrow [j, k]$;
Search the neighborhood of j and k for correlated BLIMFS with 85% proximity;
for $i \leftarrow 1$ **to** K **do**
    if $C_{coff}(i, j) \geq 0.85 * C$ **then**
        $indx \leftarrow [i]$
for $i \leftarrow 1$ **to** K **do**
    if $C_{coff}(k, i) \geq 0.85 * C$ **then**
        $indx \leftarrow [i]$
for $n \leftarrow 1$ **to** K **do**
    if $n == indx[\ ]$ **then**
        $ECG_e = BLIMF(n)$
$ECG_{esqr} \leftarrow (Square(ECG_e))$
Find peaks in ECG_{esqr}, $pk[\ ]$
Estimate the QRS complex suppressed ECG_e
for $i \leftarrow 1$ **to** *numel(pk[ ])* **do**
    $ECG_e((pk[i] - 0.06 * fs) : (pk[i] + 0.06 * fs)) = 0$
Store QRS complex suppressed ECG_e
for $n \leftarrow 1$ **to** K **do**
    if $n \neq indx[\ ]$ **then**
        $EEG_e = EEG_e + BLIMF(n)$
Estimate the artifact free EEG
$EEG_e = EEG_e + ECG_e$

Conflicts of Interest Statement

Manuscript title: Correlation-based ECG artifact removal from Single Channel EEG using Modified Variational Mode Decomposition.

The authors whose names are listed immediately below certify that they have NO affiliations with or involvement in any organization or entity with any financial interest (such as honoraria; educational grants; participation in speakers' bureaus; membership, employment, consultancies, stock ownership, or other equity interest; and expert testimony or patent-licensing arrangements), or non-financial interest (such as personal or professional relationships, affiliations, knowledge or beliefs) in the subject matter or materials discussed in this manuscript.

Author names:

1. CHINMAYEE DORA
2. PRADYUT KUMAR BISWAL

The authors whose names are listed immediately below report the following details of affiliation or involvement in an organization or entity with a financial or non-financial interest in the subject matter or materials discussed in this manuscript. Please specify the nature of the conflict on a separate sheet of paper if the space below is inadequate.

Author names:

This statement is signed by all the authors to indicate agreement that the above information is true and correct (*a photocopy of this form may be used if there are more than 10 authors*):

Author's name (typed)	Author's signature	Date
1. CHINMAYEE DORA	Chinmayee Dora.	28.02.2019
2. PRADYUT K. BISWAL	Pradyut Biswal	28/2/2019